

Optimized Double-well quantum interferometry with Gaussian squeezed-states

Y. P. Huang and M. G. Moore

Department of Physics & Astronomy, Ohio University, Athens, OH 45701

Department of Physics & Astronomy, Michigan State University, East Lansing, MI 48824

A Mach-Zehnder interferometer with a Gaussian number-squeezed input state can exhibit beyond standard-quantum-limit (SQL) phase resolution over a large range of measured phase-shifts in $(-\pi/2, \pi/2)$. For a single measurement, the smallest achievable phase uncertainty is $1.63 \tan^{1/3} |\theta|/N^{2/3}$ for nonzero phase θ . Due to the explicit θ dependence, the uncertainty converges quickly to Heisenberg scaling $\sim 1/N$ with only a few additional adaptive measurements. In contrast, previously studied input states degrade to worse than SQL for nonzero phases, and are not amenable to multiple adaptive measurement schemes. Our optimized scheme can be readily implemented in a double-well Bose-Einstein condensate system.

PACS numbers: 03.75.Dg, 03.75.Lm, 42.50.Dv

Measuring an arbitrary phase at beyond standard quantum limit (SQL) precision has been an ultimate goal in quantum interferometry [1]. It is widely accepted that smallest phase uncertainty allowed by quantum mechanics scales at $\sim 1/N_T$, the so-called Heisenberg scaling, where N_T is the total number of particles used in one or multiple measurements. This represents a $\sim \sqrt{N_T}$ improvement over SQL obtainable with classical states. There have been many proposals to achieve Heisenberg-scaling phase uncertainty, which can be grouped into two categories: interferometers with number-squeezed input states [3, 5, 6, 7] and those based on the maximally-entangled N -particle NOON state, $\frac{1}{\sqrt{2}}(|N, 0\rangle + |0, N\rangle)$ [8, 9, 10, 11]. Besides from its extreme fragility against environmental decoherence, it is now understood that the NOON state can achieve a phase uncertainty of $\Delta\theta \sim 1/N$ only if it is already known within an interval of $2\pi/N$, an evident paradox [13, 14]. Number-squeezed states, on the other hand, seem promising, although previous studies have only demonstrated Heisenberg-scaling for zero phase-shift. In this Letter we explore the use of number-squeezed states for measuring non-zero phases with greater than SQL precision.

Interestingly, the state with maximum number-squeezing, the Twin-Fock (TF) state $|N/2, N/2\rangle$, has been recently shown to be *worse* than SQL [2, 13]. This has led Pezzé and Smerzi to propose the state $\frac{1}{\sqrt{2}}(|N/2 + 1, N/2 - 1\rangle + |N/2 - 1, N/2 + 1\rangle)$, which they prove to be Heisenberg-scaling for phase $\theta = 0$. In this Letter we demonstrate that for $\theta \neq 0$, the phase-uncertainty of the Pezzé-Smerzi (PS) state rapidly decays to worse than SQL, and in the limit of large N approaches a constant value independent of N . Furthermore, this decaying can not be overcome by multiple measurement, hence the PS state is incapable of measuring an arbitrary phase. Other proposed schemes include combining squeezed states with either repeated [4] or multiple adaptive measurements [15], either apply only to zero phase or converge only very slowly towards beyond-SQL precision.

In this Letter we consider Gaussian squeezed (GS)

states of the form $|\sigma\rangle = \sum_{n=-N/2}^{N/2} \mathcal{N} e^{-n^2/4\sigma^2} |n\rangle$, where $|n\rangle = |N/2 + n, N/2 - n\rangle$ and \mathcal{N} is the normalization constant. With number-squeezing defined as $\Delta n < \sqrt{N}/2$, these states are number-squeezed for $N \gg \sigma^2$. These states can readily be created to good approximation in a double-well Bose-Josephson Junction (BJJ) system [16, 17, 18], as they are the ground state of the system. The width σ can be tuned by adiabatically varying the ratio of the collision and tunneling coefficients, either by using a Feshbach resonance, and/or varying the shape of the potential. A matter-wave interferometer configured on this system [19, 20] is an ideal candidate for high-precision measurement, including the capability for measurements at the single-particle level [21, 22].

The double-well BJJ system is described by the Hamiltonian,

$$\hat{H}(\chi) = -2\tau \hat{J}_x + \delta \hat{J}_z + U \hat{J}_z^2, \quad (1)$$

where τ is the inter-well tunneling rate, U is the atom-atom interaction strength, and δ is the asymmetric tilt of the double-well, presumably due to the external perturbation being measured. The angular momentum operators are defined as $\hat{J}_x = \frac{1}{2}(\hat{c}_L^\dagger \hat{c}_R + \hat{c}_R^\dagger \hat{c}_L)$, $\hat{J}_y = \frac{1}{2i}(\hat{c}_L^\dagger \hat{c}_R - \hat{c}_R^\dagger \hat{c}_L)$ and $\hat{J}_z = \frac{1}{2}(\hat{c}_L^\dagger \hat{c}_L - \hat{c}_R^\dagger \hat{c}_R)$, with \hat{c}_L, \hat{c}_R the annihilation operators for particles in the two localized modes labeled as L, R , respectively. For repulsive atom-atom interaction, and $\delta \approx 0$ the ground state is very close to a GS state with $\sigma^2 = N/4\sqrt{1 + UN/\tau}$ [24]. For $UN \ll \tau$ we recover the two-mode coherent state with width $\sigma = \sqrt{N}/2$, characteristic of coherent state, while for $UN \gg \tau$ the ground state becomes number-squeezed with $\sigma \approx (N\tau/U)^{1/4}/2$.

To implement a Mach-Zehnder (MZ) interferometer, we tune $U = 0$ and allow tunneling for a $\pi/4\tau$ duration, thus implementing a linear 50/50 beamsplitter, which is described by the propagator $e^{i\frac{\pi}{2}\hat{J}_x}$. This is followed by a sudden raising of the potential barrier to turn off tunneling and allow phase acquisition due to the small but non-vanishing δ . Holding the system for a measurement time

T , a phase shift of $\theta = -\delta T$ will be acquired, described by the propagator $e^{i\theta\hat{J}_z}$. The barrier is then lowered to allow another $\pi/4\tau$ -period tunneling, and the output is read by measuring the atom number difference n between the two wells.

In a MZ interferometer, the input state $|\Psi_{in}\rangle$ is transformed into the phase-dependent output state $e^{-i\theta\hat{J}_y}|\Psi_{in}\rangle$ (derived via the identity $e^{i\frac{\pi}{2}\hat{J}_x}e^{i\theta\hat{J}_z}e^{i\frac{\pi}{2}\hat{J}_x} = e^{-i\theta\hat{J}_y}e^{i\pi\hat{J}_x}$ [5]). This transformation can be intuitively described in the Bloch sphere picture [3], where, a two-mode coherent input state corresponds to a circle around $\langle\hat{J}_x\rangle = N/2$ and $\langle\hat{J}_y\rangle = \langle\hat{J}_z\rangle = 0$, while the TF state is a thin ring centered at $\langle\hat{J}_z\rangle = 0$. In between the two, GS state corresponds to an ellipse compressed along the J_z -direction. The TF and GS states are shown in figure 1(a). As these states are symmetric under $e^{i\pi\hat{J}_x}$, the transformation from input to output state is then achieved by a rotation of angle θ about the J_y -axis, as shown in figure 1 (b). Phase information is obtained by measuring number difference between the two interferometer modes, which projects the output state onto a \hat{J}_z eigenstate $|n\rangle$.

Quantum fluctuations in this measurement are constrained by the span of output distribution projected onto the J_z -axis, as shown in figure 1 (d). Due to the rigid rotation, the span's length will be determined by a θ -dependent combination of the J_x - and J_z - widths of input distribution. Thus, while the initial state can be arbitrarily compressed on one direction at the cost of being extended in another, maximum compression clearly doesn't lead to minimal number fluctuation. For the two-mode coherent state, the span is $\sim\sqrt{N}$, leading to SQL phase resolution. For the TF state, on the other hand, the span is $\sim N$ at nonzero phase, leading to worse-than-SQL resolution. The goal of this paper is thus to find the optimal squeezing to minimize the phase uncertainty for a fixed particle number N and arbitrary θ .

Before we present our numerical results from based on rigorous Bayesian analysis, we first use linearized error propagation to provide an approximate analytical description of the interferometer performance. An analytical result is important in predicting the behavior at large N , where a numerical result is difficult or unaccessible. The error propagation method is valid provided the interferometer output is a gaussian [2, 13], which is roughly true in our case. In this approach, the phase uncertainty is computed via $\Delta\theta = \left[\frac{\partial\langle\hat{J}_z\rangle}{\partial\theta}\right]^{-1}\Delta J_z$, evaluated at the interferometer output. The expectation values at the output are related to those at the input, $\langle\hat{J}_{x,z}^i\rangle$, $\Delta J_{x,z}^i$, via $\langle\hat{J}_z\rangle = \cos\theta\langle\hat{J}_z^i\rangle + \sin\theta\langle\hat{J}_x^i\rangle$ and $\Delta J_z = \sqrt{\cos^2\theta\Delta J_z^i{}^2 + \sin^2\theta\Delta J_x^i{}^2}$. These exact results fit well in geometrical intuitions in the Bloch-sphere picture, illustrated in Fig. 1 (d). With our input state, $\langle\hat{J}_x^i\rangle \approx N/2$, $\langle\hat{J}_z^i\rangle = 0$ and $\Delta J_z^i = \sigma$, which immediately leads to $\langle\hat{J}_z\rangle = N(\sin\theta)/2$. From a geometric Bloch-

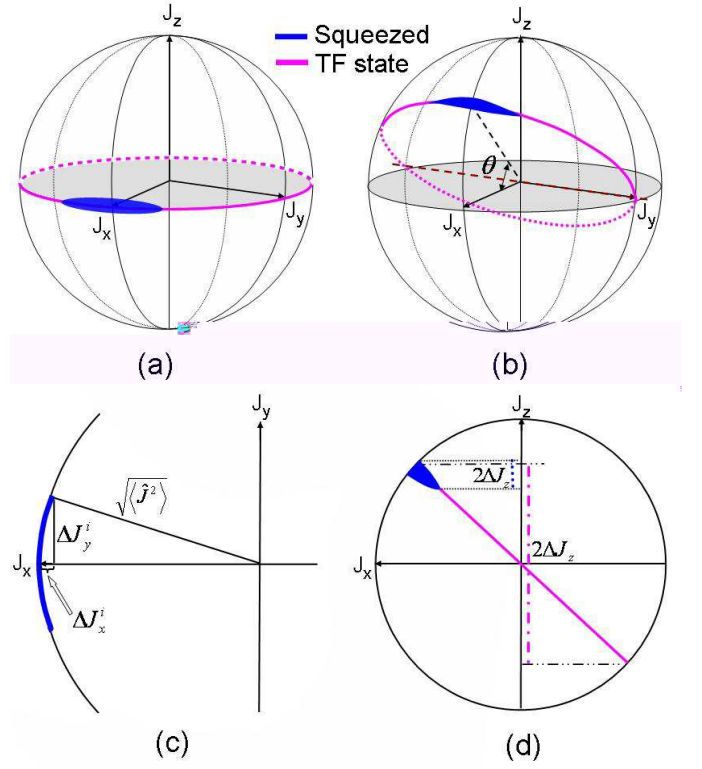


FIG. 1: (Color online) MZ interferometry in bloch sphere picture: (a) input states, where the strip, ellipse correspond to TF and GS states, respectively; (b) output states; (c) partial planform of the squeezed state from J_z -axis; (d) planform of output states from J_y -axis.

sphere analysis we find, $\Delta J_x^i = \sqrt{\langle\hat{J}^2\rangle} - \sqrt{\langle\hat{J}_z^i\rangle - \Delta J_y^i{}^2}$, as shown in figure.1 (c). With σ in current operational region ($1, \sqrt{N}/2$), our state is of minimal uncertainty with $\Delta J_y^i\Delta J_z^i = \langle\hat{J}_x^i\rangle/2$, which gives $\Delta J_y^i = N/4\sigma$. This gives $\Delta J_x^i = \alpha N/\sigma^2$, with $\alpha \approx 0.06$. An exact numerical calculation verifies the analytic form, but gives $\alpha = 0.09$. Inserting these results into the error-propagation formula, we find

$$\Delta\theta = \frac{2\sigma}{N}\sqrt{1 + \left[\frac{\alpha N \tan\theta}{\sigma^3}\right]^2}. \quad (2)$$

We now minimize the phase variance by tuning σ while holding N fixed, which leads to $\Delta\theta_{min} \approx 1.23(\tan|\theta|)^{1/3}/N^{2/3}$ at $\sigma_{min} \approx .503(N \tan|\theta|)^{1/3}$. From self-consistency, these expressions are valid only when $10/N \lesssim |\theta| \lesssim \tan^{-1}\sqrt{N} \approx \pi/2$. We note that a similar analytical result for $|\theta| \lesssim 10/N$ is lacking, because the optimal input is more like the TF state than a gaussian state, so the error propagation method becomes invalid.

We now employ rigorous Bayesian analysis to quantify the phase uncertainty and validate our approximate analytic results. According to Bayes theorem, upon a measurement result n_m , the probability that the actual

phase is ϕ is $P(\phi|n_m) = P(n_m|\phi) / \int d\theta P(n_m|\theta)$, where $P(n|\theta) = |\langle n|e^{-i\theta\hat{J}_y}|\psi_{in}\rangle|^2$. To make a theoretical performance analysis for a fixed θ , we average over all possible measurement outcomes, defining

$$P(\phi|\theta) = \sum_n P(\phi|n)P(n|\theta). \quad (3)$$

This can be interpreted as the probability for the experimentalist to infer ϕ given a true phase-shift of θ . $\Delta\theta$ is then defined as half of the interval around θ containing 68% of the total probability. From a straightforward analysis, we find that for a gaussian distribution $\Delta\theta$ computed this way is approximately $\sqrt{2}$ greater than that computed via linear error propagation.

Using this approach, we numerically find σ_{min} and $\Delta\theta_{min}$, with results shown in Fig. 2. In figure 2(a), we plot σ_{min} as a function of N for several θ s, where an asymptotical analysis reveals

$$\sigma_{min}(\theta, N) = \begin{cases} 1.00, & |\theta| < 10/N; \\ 0.45(N \tan |\theta|)^{1/3}, & |\theta| > 10/N, \end{cases} \quad (4)$$

in good agreement with our analytical result. In Fig. 2(b) we plot the corresponding $\Delta\theta_{min}$ versus N for several θ s, obtained by setting $\sigma = \sigma_{min}(\theta, N)$. It is found that asymptotically,

$$\Delta\theta_{min}(\theta, N) = \begin{cases} 3.50/N, & |\theta| < 10/N; \\ 1.63(\tan |\theta|)^{1/3}/N^{2/3}, & |\theta| > 10/N. \end{cases} \quad (5)$$

To distinguish two phases θ_1, θ_2 , requires $|\theta_1 - \theta_2| > \Delta\theta_1 + \Delta\theta_2$, which leads to $\theta = \pm 6.4/N$ as of the smallest measurable non-zero phases. Furthermore, if the measuring phase is a priori known to be within a range of $[-\theta_r, \theta_r]$, the measurement uncertainty is bounded by $\Delta\theta < \Delta\theta_{min}(\theta_r, N)$. This exhibits an $N^{1/6}$ improvement in scaling over SQL, which becomes significant only at very large N , giving a factor 10 improvement for $N = 10^6$. In many applications of high precision measurements, however, phases to be measured lie within very small intervals. In this case, our interferometer can reduce the phase uncertainty considerably even at small N , simply due to that the associated coefficient in Eq. 5, i.e., $1.63(\tan |\theta|)^{1/3}$, can be small. In contrast, the phase-uncertainty at SQL is $\Delta\theta_{SQL} = N^{-1/2}$ for all θ . This is due to the fact that stronger number-squeezing can be tolerated at small angles before the mixing in of \hat{J}_x noise becomes detrimental.

In order to measure precisely an arbitrary phase that may not be small, Heisenberg-scaling precision can still be achieved if we combine the present scheme with multiple adaptive and/or repeated measurements [5, 15]. In the method, assuming an unknown phase within interval $[-\theta_r, \theta_r]$ ($\theta_r < \pi/2$), we first perform a measurement with $\sigma = \sigma_{min}(\theta_r)$, from which a phase shift θ_1 is inferred. We then subtract θ_1 from the interferometer by

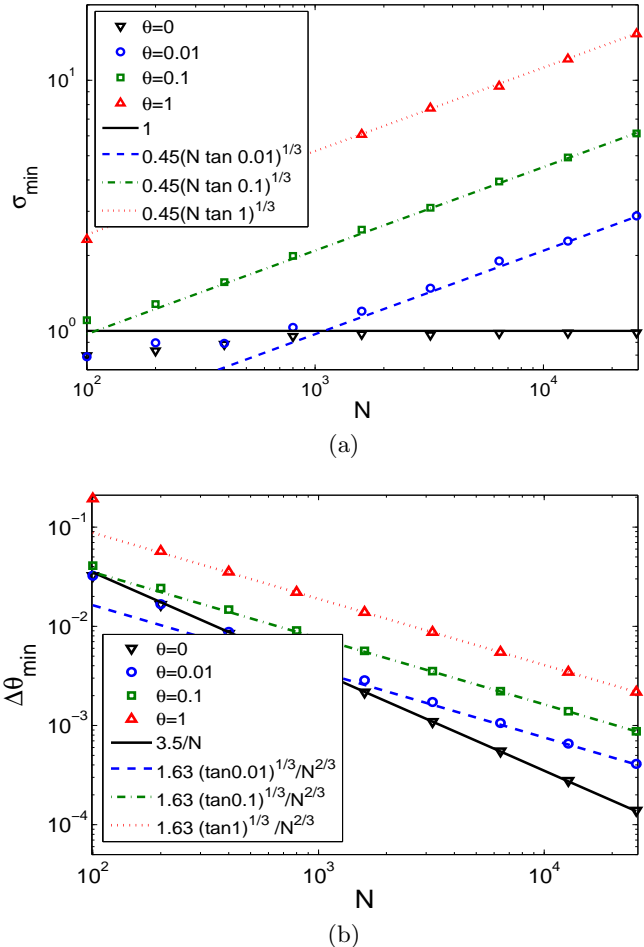


FIG. 2: (Color online) Figure (a): Optimal width σ_{min} versus N for different θ ; (b): corresponding minimal phase uncertainty. In both figures, data points represent exact numerical result, while straight lines represent asymptotical forms of Eq.(4) and Eq.(5), respectively.

adjusting the tilt δ . Afterwards, the remaining phase will be constricted within $[-\theta'_r, \theta'_r]$, where $\theta'_r = \Delta\theta_{min}(\theta_r)$. The next measurement will then be performed with $\sigma_{min}(\theta'_r)$, further reducing the phase uncertainty to less than $\Delta\theta_{min}(\theta'_r) = \Delta\theta_{min}(\Delta\theta_{min}(\theta_r))$. We keep repeating this procedure M times until the phase uncertainty is reduced to $\lesssim 10/N$, i.e., the interferometer enters the Heisenberg scaling region. This requires

$$M = 0.9 \ln[\ln N \tan \theta_r / 2.08] - 0.4. \quad (6)$$

For example, at $\theta_r = \pi/4$ and $N = 10^6$, $M = 2.2$, i.e. only two measurements are required. For $N = 10^{12}$, $M = 3.0$, requiring three measurements, six orders of magnitude improvement in the final phase-uncertainty at the cost of one additional measurement. Even for θ_r extremely close to $\pi/2$, M remains small, for example, $\theta_r = \pi/2 - 10^{-10}$ gives $M \approx 3.3$ for $N = 10^6$, and $M \approx 3.6$ for $N = 10^{12}$. Hence, for arbitrary phases in

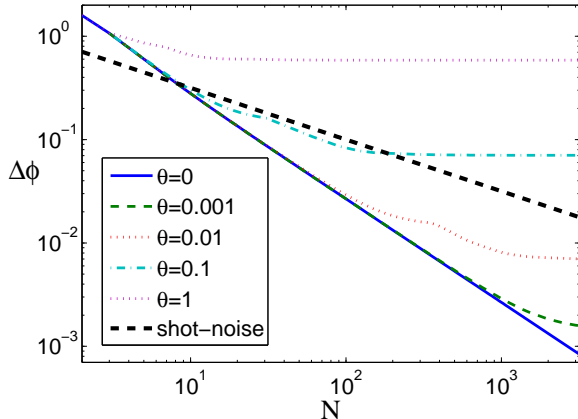


FIG. 3: (Color online) $\Delta\theta$ versus N at several phases for MZ interferometer with PS input. The thicker dashed-line represents $\Delta\theta = 1/\sqrt{N}$. In figure, since there are two symmetric peaks in $P(\phi|\theta)$, the PS interferometer is unable to distinguish between positive and negative phases. Hence, to derive a meaningful result, θ is assumed to be positive and $P(\phi|\theta)$ is truncated at $\phi = 0$, based on which $\Delta\theta$ is computed.

$(-\pi/2, \pi/2)$, our interferometer converges quickly to the Heisenberg scaling region within a few measurements, regardless of N , with the experimental value for the initial unknown phase given by $\theta = \sum_{j=1}^M \theta_j$ with a quantum-limited uncertainty of $\sim 10/N = (10M)/N_{tot}$, where $N_{tot} = MN$ is the total number of atoms employed. This gives an improvement over SQL measurements by a factor $\sim \sqrt{N}/10$.

In order to further reduce the phase uncertainty, one can then set $\sigma = 1$ and perform K additional measurements. According to Bayesian analysis, this will alter the phase distribution to $[P(\phi|\theta)]^{(1+K)}$. For quasi-gaussian distributions, the phase uncertainty is then reduced by $\sqrt{1+K}$ after K measurements. For $K \gg M$ the final phase uncertainty is then $\Delta\theta \leq 3.5\sqrt{K}/N_{tot}$, which is a factor $\sqrt{N}/3.5$ improvement over an SQL measurement with the same N_{tot} , corresponding to Heisenberg-limited behavior. In [4] it is shown that this scaling can be achieved for a wide variety of input states, but only for $\theta = 0$. We find that this will not work for $\theta \neq 0$ without the addition of an adaptive measurement scheme such as ours.

Lastly, we now show that the PS state can not surpass SQL in measuring a non-zero. This can be seen in Figure 3, where we plot the estimated phase uncertainty versus particle number N for different values of θ . We see that at $\theta = 0$, a straight line on log-log scale is found, and a least-square fitting reveals $\Delta\theta = 2.67/N$, agreeing with the previous result in Ref. [2]. However, for non-zero θ , it is seen that $\Delta\theta$ obeys a $1/N$ power law only for $N < 1/\theta$, whereas for $N > 1/\theta$, it approaches a constant N -independent value. This type of behavior would also be

seen with GS states if σ were held fixed and N increased, although the cross-over is shifted to $N = 10\sigma^3/\tan\theta$, which can be quite large for small θ and moderate σ . The saturation behavior in both cases occurs when the contribution from the \hat{J}_x^i -noise becomes larger than that from the \hat{J}_z^i -noise. Because the PS state is very similar to the TF state, this occurs immediately for $\theta \neq 0$, as seen in Fig. 1 (a). The PS state is also incompatible with multiple measurement schemes because it cannot distinguish positive from negative phases.

In conclusion, we have shown that our adaptive GS state scheme has three advantages over previously discussed MZ interferometry schemes, It (1) can readily be implemented in a double-well BEC system, (2) can achieve a resolution beyond SQL for a wide range of phases for a single measurement, and (3) quickly converges to Heisenberg scaling with only a few adaptive measurements, and reaches the Heisenberg limit with subsequent repeated measurements.

-
- [1] V. Giovannetti, S. Lloyd, and L. Maccone, *Science* **306**,1330 (2004).
 - [2] L. Pezzé and A. Smerzi, *Phys. Rev. A* **73**, 011801(R) (2006).
 - [3] K. Eckert, P. Hyllus, D. Bruß, U. V. Poulsen, M. Lewenstein, C. Jentsch, T. Müller, E. M. Rasel, and W. Ertmer, *Phys. Rev. A* **73**, 013814 (2006).
 - [4] H. Uys and P. Meystre, *Phys. Rev. A* **76**, 013804 (2007)
 - [5] B. Yurke, S. L. McCall, and J. R. Klauder, *Phys. Rev. A* **33**, 4033 (1986).
 - [6] M. J. Holland and K. Burnett, *Phys. Rev. Lett.* **71**, 1355 (1993).
 - [7] P. Bouyer and M. A. Kasevich, *Phys. Rev. A* **56**, R1083 (1997).
 - [8] J. J. Bollinger, Wayne M. Itano, D. J. Wineland, and D. J. Heinzen, *Phys. Rev. A* **54**, R4649 (1996).
 - [9] C. C. Gerry, *Phys. Rev. A* **61**, 043811,(2000)
 - [10] W. J. Munro, K. Nemoto, G. J. Milburn, S. L. Braunstein, *Phys. Rev. A* **66**, 023819 (2002)
 - [11] S. F. Huelga, C. Macchiavello, T. Pellizzari, A. K. Ekert, M. B. Plenio and J. I. Cirac, *Phys. Rev. Lett.* **79**, 3865 (1997).
 - [12] T. Kim, J. Dunningham, and K. Burnett, *Phys. Rev. A* **72**, 055801 (2005).
 - [13] Z. Hradil and J. Řeháček, *Phys. Lett. A* **334**, 267 (2005).
 - [14] L. Pezzé and A. Smerzi, e-print quant-ph/0508158 (2005).
 - [15] D. Denot, T. Bschorr, and M. Freyberger, *Phys. Rev. A* **73**, 013824 (2006).
 - [16] T. Schumm, S. Hofferberth, L. M. Andersson, S. Wildermuth, S. Groth, I. Bar-Joseph, J. Schmiedmayer and P. Krüger, *Nature Physics* **1**, 57 (2005).
 - [17] R. Gati, M. Albiez, J. Fölling, B. Hemmerling, and M. K. Oberthaler, *Appl. Phys. B* **82** 207 (2006).
 - [18] G. -B. Jo *et al.*, *Phys. Rev. Lett.* **98** 030407 (2007).
 - [19] C. Lee, *Phys. Rev. Lett.* **97**, 150402 (2006)
 - [20] L. Pezzé, A. Smerzi, G. P. Berman, A. R. Bishop, and L. A. Collins, *Phys. Rev. A* **74**, 033610 (2006).

- [21] M. Saba, T. A. Pasquini, C. Sanner, Y. Shin, W. Ketterle, and D. E. Pritchard, *Science* **307**, 1945 (2005)
- [22] C.-S. Chuu, F. Schreck, T. P. Meyrath, J. L. Hanssen, G. N. Price, and M. G. Raizen, *Phys. Rev. Lett.* **95**, 260403 (2005).
- [23] C. M. Caves, C. A. Fuchs, and R. Schack, *Phys. Rev. A* **65**, 022305, (2002)
- [24] A. Imamoglu, M. Lewenstein, and L. You, *Phys. Rev. Lett.* **78** 2511 (1997).